Citation: Cueva, J., K. Kusunoki (2022), Estimation of the equivalent damping ratio for low energy dissipation systems under mainshock-aftershock sequences to determine the damage level, Synopsis of IISEE-GRIPS Master's Thesis.

ESTIMATION OF THE EQUIVALENT DAMPING RATIO FOR LOW ENERGY DISSIPATION SYSTEMS UNDER MAINSHOCK-AFTERSHOCK SEQUENCES TO DETERMINE THE DAMAGE LEVEL

Jean Cueva[1] **Supervisor: Koichi KUSUNOKI**[2]
MEE21709

ABSTRACT

The assessment of Reinforced Concrete (RC) buildings, considering mainshock-aftershock (MA) sequences, has been addressed in previous studies in which the main objective is to predict the damage level after a maximum expected aftershock and then judge if the building can continue operating or not. This study uses numerical simulations to determine the equivalent damping ratio for structures with low energy dissipation and under mainshock-aftershock sequences and using several Single Degree of Freedom (SDOF) systems with different hysteresis models.

Results indicate the variation of the damping ratio for each hysteresis model, and the higher and lower values correspond to the Degrading trilinear and Origin-oriented models, respectively. In addition, the parameter a_2, which is defined as the ratio of the yielding stiffness to the elastic stiffness of the capacity curve, presents a significant influence on the equivalent damping ratio. For that reason, in the beginning, this study presented a new expression to determine the damping ratio, which considered new reduction factor values "γ" and a new coefficient to quantify the additional damping ratio due to the damage before yielding point "b," both were determined for specific values of the parameter a_2.

Due to the high values and the uncertainty of coefficient "b," the new expression was reduced for practical purposes during the mainshock and aftershock. Additionally, the damage level (ductility) for the maximum expected aftershock, and using the new "γ" values, presented a lower error percentage than the previous studies, which considered γ equal to 0.06.

Keywords: RC buildings, damping ratio, mainshock, aftershock.

1. INTRODUCTION

Although the magnitude of an earthquake is the first indicator of the level of damage to which our buildings will be subjected, it is not always the main one. In many cases, the cumulative damage due to the mainshock and subsequent aftershocks ends up being a factor that increases the risk of collapse of the buildings and compromises their functionality. Due to those mentioned above, it is essential to know the state of the building after each seismic event to know its residual capacity and thus decide whether it can be occupied immediately or not. The rapid inspection of buildings becomes more critical in essential facilities, such as hospitals, where their operability must be confirmed after each specific event due to their service. The rapid inspection method in Japan is based on a method to evaluate the residual seismic capacity index "R," defined as the ratio of the residual seismic capacity to the original capacity. A new method for assessing the real-time residual seismic capacity of existing structures using

[1] Japan-Peru Center for Earthquake Engineering Research and Disaster Mitigation (CISMID), Peru.
[2] Professor, Tokyo University.

accelerometers is part of the recent studies based on Structural Health Monitoring (SHM). This methodology uses the double integral with a wavelet transform and obtains the capacity curve of the building from the acceleration measurement in the installed sensors (Pan & Kusunoki, 2020). In addition, a study complementary to the previous one is the aftershock damage prediction of reinforced-concrete buildings using sensors, where the predicted maximum response during the Mainshock-aftershock sequence is obtained from the Capacity Spectrum Method (CSM).

2. METHODOLOGY

2.1. Performance-based procedure

The Performance-based procedure or Capacity Spectrum Method (CSM) defines a demand and capacity curve and is widely used to evaluate the performance of existing buildings as new ones (ATC-40, 1996). The demand curve represents the earthquake ground motion, and the capacity curve is presented through skeleton or primary curves and shows representative displacements and restoring forces under monotonically increasing loading.

The total damping ratio (h) is the sum of the equivalent and initial damping ratio h_0 and can be written as Equation (1) as presented in (MLIT, 2000). In addition, the value of h_{eq} is ductility dependent and takes different values during a mainshock or aftershock. For mainshocks, the reduction factor γ takes values of 0.25 and 0.20 (MLIT, 2000), and for aftershocks, new values of coefficient γ were proposed (Kusunoki, 2006) and are between 0.06 and 0.10.

$$h = \gamma\left(1 - \frac{1}{\sqrt{\mu}}\right) + h_0 \qquad (1)$$

The response reduction factor F_h is the ratio between the maximum inelastic response and the elastic spectral response for a specific effective period (T_m), which is ductility dependent. The response reduction factor, in terms of total damping ratio, Equation (2), is presented in Equation (3) (MLIT, 2000).

$$h = h_{eq} + h_0 \qquad (2) \qquad\qquad F_h = \frac{1.5}{1+10\cdot h} \qquad (3)$$

2.2. Seismic evaluation for the Mainshock-Aftershock sequence

The maximum considered aftershock is the same as the mainshock for the life-safety limit state. This condition is part of considering the most harmful scenario, where the energy released by the largest aftershock is relatively close to the mainshock. Therefore, the total ground motion is composed of wave Level-1, which corresponds to the mainshock, and wave Level-2, which corresponds to the expected aftershock, equal to the mainshock. The procedure for the numerical simulation is divided into two parts. First, determine the MA sequence for a ductility target during the mainshock. Second, the non-linear time history analysis response will be determined using the MA sequence defined in the first part. Then, the equivalent damping ratio h_{eq} and response reduction factor F_h for Mainshock (Level-1) and Aftershock (Level-2) are obtained for each Single Degree of Freedom (SDOF) system and specifics input ground motions.

3. DATA

3.1. Inelastic restoring forces models

Depending on each model, the inelastic restoring force is defined as the relation between the representative restoring force and displacement and following specific hysteresis rules. Four hysteresis models were used in this investigation: Degrading trilinear model, Origin-oriented model, Takeda model, and Takeda-slip model, and were selected to represent the systems with low energy dissipation.

Previously, the primary curve, resistance-displacement relation, under monotonically increasing loading is presented as a trilinear skeleton curve, as is illustrated in Figure 1.

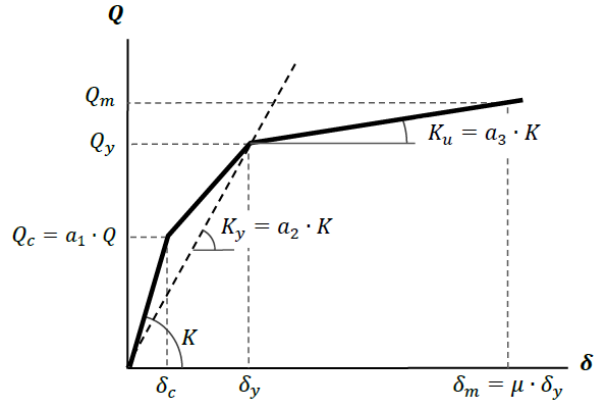

Figure 1. Primary curve (Trilinear).

Source: (Diaz, 2013).

Where:

δ_c: Displacement at cracking resistance.

δ_c: Displacement at cracking resistance.

a_1: Ratio of the cracking resistance to the yielding resistance (Q_c/Q_y).

a_2: Ratio of the yielding stiffness to the elastic stiffness (K_y/K).

a_3: Ratio of the post-yielding stiffness to the elastic stiffness (K_u/K).

3.2. Parameters

For the numerical simulation, many parameters were defined to cover as many cases as possible, both in the capacity and demand curve. The capacity curve was obtained from the Primary Curve, Figure 1, and for this research, some parameters are listed in Table 1, indicating the range of periods T and ductility targets μ.

Table 1. List of parameters for the capacity curve.

Parameter	Values
T	0.2 to 1.2 @0.2s (6 combinations)
a_1	0.2 to 0.6 @0.1 (5 combinations)
a_2	0.25 to 0.85 @0.15 (5 combinations)
a_3	0.001
μ	1 to 5 @1 (5 combinations)

For the Demand curve, ten artificial waves (Okawa, 1998) and ten earthquake records were used as input ground motions in the numerical simulations, and also, all used waves have 50Hz as sampling.

3.3. Numerical model

The new proposal for calculating the equivalent damping ratio, considering new γ values, will be applied to a numerical model, a 2D RC frame structure with six stories and two bays. The non-linear pushover analysis will be performed using the software STERA3D (Saito, 2015). The displacement versus shear curve for each story will be used as an output to convert the model into an SDOF system and apply the Capacity Spectrum Method (CSM) and Non-linear Time History Analysis (NLTHA).

4. RESULTS AND DISCUSSION

4.1. Influence of parameter a_2 in the equivalent damping ratio

The theoretically equivalent damping ratio of each model clearly shows the influence of parameter a_2, and it can be seen in cases where ductility is equal to one because values of h_{eq} higher than zero at this

yielding point indicates an additional damping ratio due to the damage after the cracking and before the yielding point, Figure 2; from now on, this additional damping ratio will be known as "b".

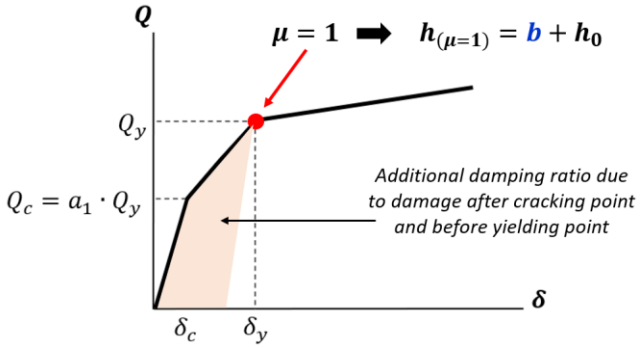

New expression to curve fitting the numerical results, ductility versus damping ratio:

$$h = \left(\gamma\left(1 - \frac{1}{\sqrt{\mu}}\right) + \boldsymbol{b}\right) + h_0 \qquad (4)$$

Figure 2. Additional damping ratio "b".

From those mentioned above and the theoretical values, the parameter a_2 was used as a variable to disaggregate the numerical results, ductility versus damping ratio, into the range of values defined in Table 1. In each group, the data were fitted to a new expression (4), similar to the one currently used (MLIT, 2000), but includes the parameter "b," and applied during the mainshock and aftershock.

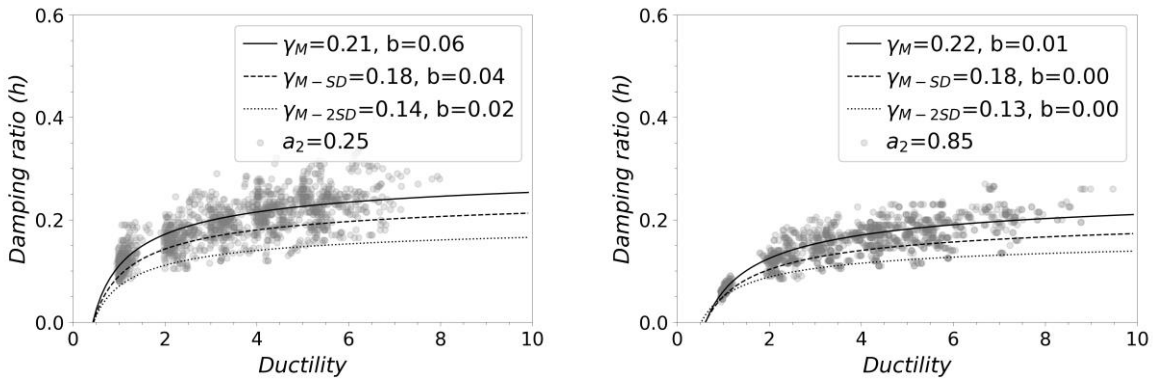

(a) $a_2 = 0.25$ (b) $a_2 = 0.85$

Figure 3. $h - \mu$ relationship during Aftershock for $a_2 = 0.25$ and $a_2 = 0.85$ (Takeda slip).

Additionally, Figure 3 (a), and (b) are presented as part of the result disaggregation during the aftershock. These graphs include a new value of γ, and "b" for the 50th percentile (γ_M), 16th percentile (γ_{M-SD}), and finally, 2.5th percentile (γ_{M-2SD}), which corresponds to the median minus two-time standard deviation. For the following procedure, the lower limit, which corresponds to the median minus two standard deviations (2.5th percentile), will be used for the new expression of calculating the damping ratio. Table 2 summarizes the γ, and b values, respectively, during the aftershock and for the 2.5th percentile.

Table 2. The γ and b values during aftershock for the 2.5th percentile.

Model	$a_2 = 0.25$		$a_2 = 0.40$		$a_2 = 0.55$		$a_2 = 0.70$		$a_2 = 0.85$	
	γ	b	γ	b	γ	b	γ	b	γ	b
Degrading trilinear	0.04	0.08	0.03	0.06	0.03	0.05	0.02	0.03	0.02	0.01
Origin oriented	0.07	0.00	0.05	0.00	0.04	0.00	0.02	0.00	0.03	0.00
Takeda	0.08	0.03	0.10	0.02	0.13	0.00	0.12	0.00	0.13	0.00
Takeda slip	0.14	0.02	0.12	0.02	0.13	0.01	0.12	0.01	0.13	0.00

4.2. Proposal of New reduction factors

Table 2 presents b values during the aftershock; and as can be seen in some models and values of parameters a_2, the coefficient b takes high values. Such condition may not occur in reality, and in that sense, it is necessary to adjust the above Expression (4), ignoring coefficient b for practical purposes. In summary, an already known equation will be used to determine the damping ratio but considering new γ values for each hysteresis model as presented in Expression (5) during the aftershock and the same during the mainshock. The γ values obtained during mainshock (γ_{ms}) and aftershock (γ_{as}) were selected for each hysteresis model to propose a linear regression and Table 3 shows the new expressions to determine the reduction factor during the mainshock and aftershock independently.

$$h = \gamma_{as}\left(1 - \frac{1}{\sqrt{\mu}}\right) + h_0 \tag{5}$$

Table 3. Reduction factor during the mainshock γ_{ms} and aftershock γ_{as}.

Model	Mainshock	Aftershock
Degrading trilinear	$\gamma_{ms} = -0.047 + 0.060(a_2)$	$\gamma_{as} = -0.033 + 0.046(a_2)$
Origin oriented	$\gamma_{ms} = -0.053 + 0.075(a_2)$	$\gamma_{as} = -0.073 + 0.082(a_2)$
Takeda	$\gamma_{ms} = 0.067 + 0.133(a_2)$	$\gamma_{as} = 0.080 + 0.068(a_2)$
Takeda slip	$\gamma_{ms} = 0.027 + 0.149(a_2)$	$\gamma_{as} = -0.013 + 0.135(a_2)$

4.3. Proposal of New reduction factors

The 2D RC Frame numerical model was converted into an SDOF system, and the capacity Spectrum and Primary Curve were obtained. The SDOF model parameters are presented in Table 4, and the reduction factor during the mainshock and aftershock and for the specific a_2 are shown in Table 5.

Table 4. Parameters of SDOF system.

Parameters
$T = 0.77\ s$
$Q_c = 261.78\ kN$
$Q_y = 858.88\ kN$
$a_1 = 0.305,\ a_2 = 0.276$

Table 5. The reduction factor γ for the equivalent SDOF system

Model	Mainshock	Aftershock
Takeda	$\gamma_{ms} = 0.15$	$\gamma_{as} = 0.09$
Takeda slip	$\gamma_{ms} = 0.16$	$\gamma_{as} = 0.13$

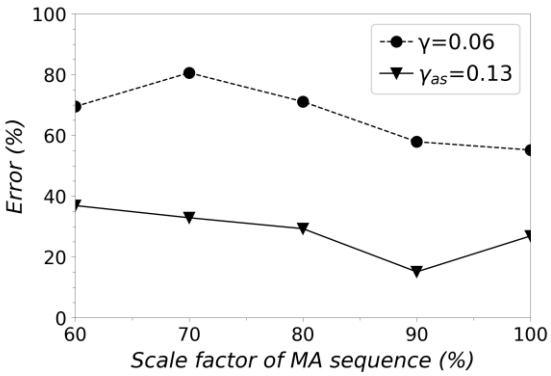

Figure 4. Comparison of the $\%error$ "wg60" and Takeda slip model.

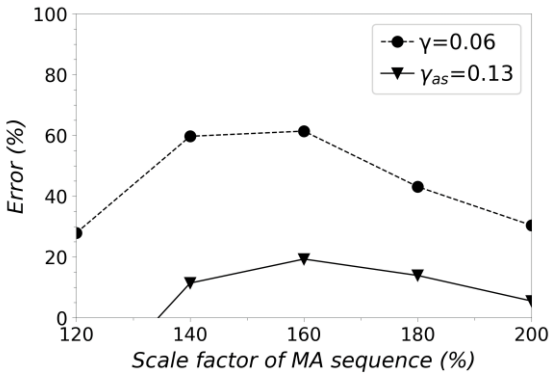

Figure 5. Comparison of the $\%error$ "El Centro EW" and Takeda slip model.

Finally, the $\%error$, between the CSM and NLTHA, for the Takeda Slip model is presented for one artificial wave "wg60" and one earthquake record "El Centro EW" in Figure 4 and Figure 5, respectively. These graphs show the difference using γ equals to 0.06 compared with the results considering the new reduction factor γ_{as} during the aftershock.

5. CONCLUSIONS

For practical uses of the new expression to determine the damping ratio (h), the coefficient b is ignored because it takes high values. This condition, high values of b, may not occur in reality because the accumulative damage and additional damping ratio at the yielding point cannot be determined theoretically. In that sense, it is necessary to adjust the new expression, ignoring the b coefficient due to the uncertainty and being reduced to the expression indicated by MLIT but using the reduction factors γ determined in this study during the mainshock and aftershock.

The present study shows more accuracy in the determination of the damping ratio during the aftershock and considering the influence of the parameter a_2, which comes from the definition of a trilinear Primary Curve and using a hysteresis model representing systems with low energy dissipation. Additionally, the procedure is summarized as follows, after defining a_2 from the Capacity Curve, the damping ratio ($h = \gamma_{as} \cdot (1 - 1/\sqrt{\mu}) + 0.05$) is obtained using a new reduction factor during the aftershock (γ_{as}) to obtain the response reduction factor ($F_h = 1.5/(1 + 10 \cdot h)$), the same expression as presented by MLIT, and finally, determine the damage level for the maximum expected aftershock.

ACKNOWLEDGMENT

I would like to express my gratitude to my supervisor Dr. Koichi Kusunoki and advisor Dr. Haruhiko Suwada for their valuable comments and their guidance throughout the process of this investigation. In addition, I would like to thank Dr. Carlos Zavala and Dr. Miguel Diaz from CISMID for their support and comments in each meeting.

REFERENCES

ATC-40. (1996). *Seismic Evaluation and Retrofit of Concrete Buildings: Vol. Report No. SS96-01*. Applied Technology Council, California.

Diaz, M. (2013). *Development of the Seismic Performance Estimation during an Aftershock considering the Equivalent Damping Ratio and the Response Reduction Ratio* [Dr. Thesis]. Yokohama National University.

Diaz, M., Gibu, P., Estacio, L., & Proano, R. (2014). Implementation of Building Monitoring Network in Peru Under SATREPS Project. *Journal of Disaster Research*, *9*(6), 1001–1007. https://doi.org/10.20965/JDR.2014.P1001

Kuramoto, H., Teshigawara, M., Okuzono, T., Koshika, N., Takayama, M., & Hori, T. (2000). *Predicting the earthquake response of building using equivalent single degree of freedom system*.

Kusunoki, K. (2006). Analytical Study on Estimation of Equivalent Viscous Damping Ratio for aftershock. *Proceedings of the Japan Concrete Institute. In Japanese*, *28*(2), 1057–1062.

Ministry of Land, I. T. and T. (MLIT). (2000). *Notification No. 1457-6: Technical Standard for Structural Calculation of Response and Limit Strength of Buildings*.

Pan, H., & Kusunoki, K. (2020). Aftershock damage prediction of reinforced-concrete buildings using capacity spectrum assessments. *Soil Dynamics and Earthquake Engineering*, *129*, 105952. https://doi.org/10.1016/J.SOILDYN.2019.105952

Saito, T. (2015). *STERA 3D User Manual version 11.0*.